applied optics

Spectral phase effects and control requirements of coherent beam combining for ultrashort ultrahigh intensity laser systems

Yong Cui,[1] Yan-qi Gao,[1,2,*] Ze-xi Zhao,[1] Zhong-yang Xu,[1] Ning An,[1] Da-wei Li,[3] Jian-wei Yu,[3] Tao Wang,[1] Guang Xu,[3] Wei-xin Ma,[1] and Ya-ping Dai[4]

[1]Shanghai Institute of Laser Plasma, 1129 Chenjiashan Road, Jiading, Shanghai 201800, China
[2]IFSA Collaborative Innovation Center, Shanghai Jiao Tong University, Shanghai 200240, China
[3]Shanghai Institute of Optics and Fine Mechanics, 390 Qinghe Road, Jiading, Shanghai 201800, China
[4]Laser Fusion Research Center, P.O. Box 919-981, Mianyang, Sichuan 621900, China
*Corresponding author: liufenggyq@siom.ac.cn

Received 2 September 2016; revised 10 November 2016; accepted 12 November 2016; posted 14 November 2016 (Doc. ID 274830); published 9 December 2016

Based on the premise that further improvements to the size and damage threshold of large-aperture optical components are severely limited, coherent beam combining (CBC) is a promising way to scale up the available peak power of pulses for ultrashort ultrahigh intensity laser systems. Spectral phase effects are important issues and have a significant impact on the performance of CBC. In this work, we analyze systematically factors such as spectral dispersions and longitudinal chromatism, and get the general spectral phase control requirements of CBC for ultrashort ultrahigh intensity laser systems. It is demonstrated that different orders of dispersion influence intensity shape of the combined beam, and high-order dispersions affect the temporal contrast of the combined beam, while the number of the channels to be combined has little impact on the temporal Strehl ratio (SR) of the combined beam. In addition, longitudinal chromatism should be controlled effectively since it has a detrimental effect on the combined beam at the focal plane, both temporally and spatially.

OCIS codes: (140.3298) Laser beam combining; (140.7090) Ultrafast lasers; (220.4830) Systems design.

https://doi.org/10.1364/AO.55.010124

1. INTRODUCTION

In recent years, there is a growing interest in creation of ultrashort ultrahigh intensity laser systems [1,2]. The ultrarelativistic intensity conditions ($>10^{23}$ W/cm^2) in these systems provide great opportunity for investigation and application of many research fields, such as laser-plasma electron and ion acceleration, hard x-ray and radiation generation, relativistic self-focusing, and so on [3,4]. To this day, the maximum available intensity for a single laser is about 2×10^{22} W/cm^2. Owing to that the peak power of a single laser source is restricted by an optical element aperture, damage threshold of materials, a thermo-optical issue, and a detrimental nonlinear effect, it is difficult to further increase the peak intensity of a single channel laser system greatly. For example, the planned peak intensities in the systems of Apollo-10P and Vulcan 10P are 10^{23}–10^{24} W/cm^2 [2,5].

Coherent beam combining (CBC) is the most promising way to scale up the available peak power while preserving the beam quality of individual laser systems, and high peak power is just the constant pursuit of ultrashort ultrahigh intensity pulse systems [6,7]. All approaches of CBC could be divided into two groups: tiled-aperture combining and filled-aperture combining. According to the former all beams are placed side by side and simultaneously combined in the focal plane of the focusing element. In the latter all beams are overlapped on beam splitters, polarizers, or dichroic mirrors.

Coherent combining of amplified laser beams was first implemented for continuous wave (CW) lasers and a long pulsed regime where thermal problems dominate. Recently, it has been extended to a short pulsed regime, namely picosecond pulses and even femtosecond pulses, including the combining of pulses amplified in fiber amplifiers and in bulk active media (laser or parametric amplification) [6,8,9]. In large-aperture ultrashort ultrahigh intensity laser systems, CBC is strongly demanded due to the urgent need for higher peak power density and severe constraints of optical elements' size and damage threshold. CBC is already planned to be used in large international facilities such as advanced radiographic

capability (ARC), petawatt aquitaine laser (PETAL), fast ignition realization experiment (FIREX), extreme light infrastructure (ELI), and exawatt center for extreme light studies (XCELS) [10,11]. Many important techniques such as phase measurements and controls, synchronization measurements and controls, and longitudinal chromatism measurements and compensations have been developed. However, there is still a great challenge to realize efficient CBC for large-aperture ultrashort ultrahigh intensity pulse laser systems, including coherent combining theories, error measurements, and controls.

In the theoretical investigation of CBC, the impact of spatial aspects such as random tilts and offset on the combining efficiency was estimated [12]. Leshchenko investigated the dependence of the combining efficiency on different misalignments and the number of combining pulses [13]. Our group has studied the spatial phase control requirements of CBC for ignition scale facilities and large-aperture ultrashort ultrahigh intensity laser facilities systematically [14,15]. Klenke *et al.* studied the impact of temporal and spectral effects such as self-phase modulation and dispersion between the pulses [16]. However, the above-mentioned investigations mainly focus on the aspects of spatial physical parameters about wave front or some temporal characteristics of pulses for CBC. The systematical theories of temporal and spectral aspects for beam combining are minimal [17,18]. These important problems should be of concern and solved primarily when CBC develops toward combining of large-aperture ultrashort ultrahigh intensity laser systems.

To understand spectral phase effects and get the control requirements of CBC for ultrashort ultrahigh intensity laser systems, we analyzed the fundamental physical process of CBC systematically in a temporal-spectral domain and revealed fundamental physical factors referred to the CBC process in this paper. Based on the physical analysis, we investigated the influence mechanism and level of the above fundamental factors for efficient CBC of ultrashort laser systems systematically. Finally, we give the core control requirements of factors in typical ultrashort pulse CBC systems. It is noted that a nonlinear spectral phase such as self-phase modulation is not the scope of this paper, owing to many discussions in former literature, where it has been confirmed experimentally that for low nonlinearity systems with $B < \pi$, this effect is negligible [18–20]. The paper is organized as follows. In Section 2 we lay out the basic principles of coherent combining for ultrashort pulse laser systems. In Section 3, we analyze the effects of spectral factors on the combining result and report spectral phase control requirements of efficient CBC for ultrashort pulses. In Section 4, we investigate the space–time effects on coherent combining results. Section 5 is the conclusion of this work.

2. THEORETICAL MODEL

In this section, we lay out basic considerations in ultrashort optical pulses to describe coherent combining of ultrashort pulses. Then we examine theoretically how spectral factors influence the performance of a combined pulse. The main difference between coherent combining in an ultrashort pulse and CW regime is that the spectrum of an ultrashort pulse extends over a large bandwidth. Therefore, excellent coherent combining of ultrashort pulses needs a spectral phase matching over the whole optical bandwidth. The spatial effects considered in CBC of CW and pulsed laser are the same. Because of this, we concentrate on spectral aspects, while assuming all beams have the same perfect spatial phase and thus leaving aside the spatial phase differences of them.

The electric field in the frequency domain can be expressed as

$$E(\omega) = A(\omega)\exp[i\phi(\omega)], \tag{1}$$

where $A(\omega)$ is the spectral amplitude and $\phi(\omega)$ is the spectral phase. For a Gaussian spectral amplitude,

$$A(\omega) = \exp\left[-2\ln 2\left(\frac{\omega-\omega_0}{\omega_{\mathrm{FWHM}}}\right)^2\right], \tag{2}$$

where ω_{FWHM} is the full width at half-maximum (FWHM) of the spectral intensity and ω_0 is the central angular frequency of the ultrashort pulse. It is customary to expand the spectral phase $\phi(\omega)$ in the Taylor series around the central angular frequency ω_0 as [21]

$$\phi(\omega) = \phi(\omega_0) + \phi'(\omega_0)(\omega-\omega_0) + \frac{1}{2}\phi''(\omega_0)(\omega-\omega_0)^2 + \frac{1}{6}\phi'''(\omega_0)(\omega-\omega_0)^3 + \frac{1}{24}\phi''''(\omega_0)(\omega-\omega_0)^4 + \ldots, \tag{3}$$

where $\phi(\omega_0)$ is the absolute phase, corresponding to a piston, and $\phi'(\omega_0)$ is the first-order phase, corresponding to a group delay (GD). $\phi''(\omega_0)$ is the second-order phase, representing a group delay dispersion (GDD) or linear chirp. $\phi'''(\omega_0)$ is the third-order dispersion (TOD), and $\phi''''(\omega_0)$ is the fourth-order dispersion (FOD). Higher-order dispersions are neglected here.

An ultrashort pulse is described as a complex envelope $E(t)$ in the time domain and can be expressed as the inverse Fourier transformed of $E(\omega)$,

$$E(t) = \Im^{-1}[E(\omega)]. \tag{4}$$

When dispersion of up to the second order is considered, Eq. (4) is readily solved by using the Fourier-transform technique,

$$E(t) = \sqrt{\frac{\tau^2}{\tau^2 - 4\ln 2\cdot\phi''(\omega_0)i}} \cdot \exp\left\{i\omega_0 t + \phi(\omega_0) - \frac{2\ln 2[t+\phi'(\omega_0)]^2}{\tau^2 - 4\ln 2\cdot\phi''(\omega_0)i}\right\}, \tag{5}$$

where $\tau(\tau = 4\ln 2/\omega_{\mathrm{FWHM}})$ is the FWHM of transform-limited pulse width.

When only the TOD is considered, an analytic solution can be written in terms of the Airy function as [22]

$$E(t) = \sqrt{\frac{\pi\tau^2}{2\ln 2}}\cdot\left(\frac{2}{\phi'''(\omega_0)}\right)^{\frac{1}{3}} \times \exp\left\{\frac{\tau^6}{192\cdot(\ln 2)^3\cdot[\phi'''(\omega_0)]^2} - \frac{\tau^2 t}{4\ln 2\cdot\phi'''(\omega_0)}\right\} \cdot Ai\left\{\left(\frac{\tau^2}{8\ln 2}\right)^2\cdot\left[\frac{\phi'''(\omega_0)}{2}\right]^{-\frac{4}{3}} \cdot\left[1 - \frac{32\cdot(\ln 2)^2\phi'''(\omega_0)t}{\tau^4}\right]\right\}. \tag{6}$$

It is unrealistic to find an analytic solution similar to Eq. (5) when FOD is referred, so instead the electric field could be numerically modeled with the fast Fourier transform algorithm.

To analyze and understand spectral phase effects on a carrier wave and envelope of pulse, we take a Gaussian pulse with duration of 5 fs and central wavelength of 800 nm, for example. The results of the electric field calculation based on Eqs. (1)–(6) are shown in Fig. 1. As shown in Fig. 1(a), $\phi(\omega_0)$ is simply a constant parameter, namely a piston, and here we assume all beams have the same piston. Group delay gives the retardation of the pulse in time and does not change the shape of the pulse. The reason is that the spectral phase changes with angular frequency linearly, and it is similar to the phase introduced by propagation in vacuum, as is shown in Fig. 1(b). It is obvious that group delay $\phi'(\omega_0)$ of pulses to be coherent combined should be the same so that the pulses arrive simultaneously at the combining component. In Fig. 1(c), GDD changes the phase of each spectral component of the pulse and thus modifies the pulse shape. The pulse duration mainly depends on GDD. The reason is that different frequency components of a pulse travel at different speeds. The time delay in the arrival of different spectral components leads to pulse broadening and peak power decreasing. Compared to GDD, higher-order dispersions have little impact on the pulse duration, but they influence the shape and contrast ratio of pulse significantly, according to Figs. 1(d) and 1(e). TOD results in asymmetry in the pulse with an oscillatory structure near one of its edges, depending on the sign of TOD, while FOD makes both the leading and trailing edge of the pulse less steep and thus introduces unwanted pedestals on the pulse.

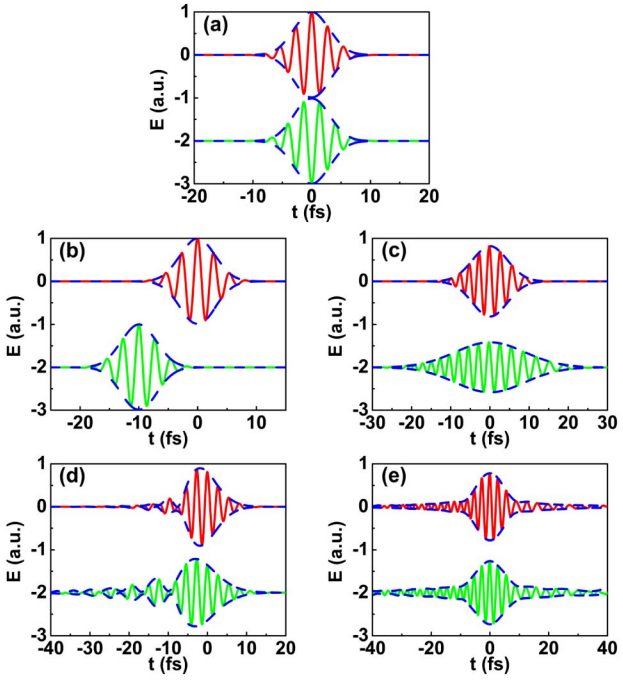

Fig. 1. Schematic temporal effect of the spectral phase derivatives, $\phi(\omega_0)$ (a), GD (b), GDD (c), TOD (d), and FOD (e). The red and green continuous lines denote the carrier wave of the electric field, and the blue-dashed line denotes the envelop of the electric field.

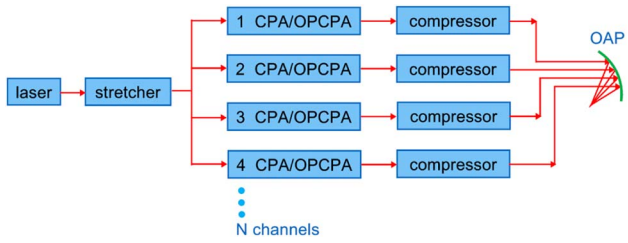

Fig. 2. General setup of ultrashort ultrahigh intensity laser system based on CBC.

Figure 2 is the general scheme of a large-aperture ultrashort ultrahigh intensity laser system based on tiled-aperture CBC, which is much more promising for achieving high peak intensity. Temporally stretched pulses are divided into N channels and amplified independently in respective channels based on chirped pulse amplification (CPA) or optical parametric chirped pulse amplification (OPCPA). After compression all pulses are coherently added in the focal plane of an off-axis parabolic mirror (OAP) to form the combined beam with high peak intensity. The processes of stretching, amplification, and compression in every channel all contribute to the dispersion of systems. Assuming there are ultrashort pulses of N channels to be combined, as shown in Fig. 2, the electric field of the combined pulse can be written as

$$E_{\mathrm{CBC}}(t) = \sum_{n=1}^{N} E_n(t). \tag{7}$$

The intensity of the combined pulse can be expressed as

$$I_{\mathrm{CBC}}(t) = |E_{\mathrm{CBC}}(t)|^2 = \left|\sum_{n=1}^{N} E_n(t)\right|^2 = \left|\sum_{n=1}^{N} \Im^{-1}[E_n(\omega)]\right|^2. \tag{8}$$

Thus the temporal Strehl ratio (SR) of the combined pulse is given by

$$\mathrm{SR} = \frac{\max(I_{\mathrm{CBC}}(t))}{\max(I_{\mathrm{CBC}}^{\mathrm{ideal}}(t))}, \tag{9}$$

where $I_{\mathrm{CBC}}^{\mathrm{ideal}}(t)$ is the ideal intensity of the combined beam achievable when combining coherent beams with no residual dispersions. Expressions (8) and (9) are the basic principles for the calculation of CBC. It reveals the importance of the relative spectral phase among the electric fields of N channels to be combined.

3. DISPERSION

From the above discussion, it is clear that dispersions of different orders influence a pulse's arriving time and temporal shape. So, for CBC the individual pulse's dispersion and the dispersion difference among pulses to be combined both contribute to the final combined pulse's temporal characteristics. In this section, based on the theory analysis in Section 2, we explore how dispersion characteristics of individual beams and dispersion differences among pulses influence CBC by numerical simulation, and then we give the guideline of dispersion control requirements of CBC for ultrashort pulses.

For an ultrashort ultrahigh intensity laser system, the FWHM of the spectral intensity bandwidth is assumed to be 32 nm, corresponding to pulses with transform-limited pulse duration as short as 30 fs. Then we extend the particular case to general ones and give the control requirements for CBC of pulses with other durations. It should be noticed that the simulation results are independent on the center wavelength of the system, for the absolute phase $\phi(\omega_0)$ is not considered here. In the following numerical simulation, when one dispersion term is considered, other dispersion terms will be neglected.

A. Control Requirement for the Individual Pulse's Own Dispersion

To simplify the analysis, numerical simulation for CBC of two channels is considered first, and the individual beams have the same dispersion. The group delay does not influence the individual pulse's shape but only changes the arrival time of the pulse, so it has nothing to do with the temporal SR of the individual pulse. If the two pulses have the same group delay, namely they arrive at the combining component simultaneously, the temporal SR of the combined pulse is always 1.

According to Eq. (9), we numerically modeled the effects of GDD, TOD, and FOD on the combined pulse's temporal SR and pulse contrast, defined as the ratio of the peak intensity with respect to the parasitic structures such as prepulses and pedestals of the pulse. The temporal SR of the combined pulse as a function of GDD, TOD, and FOD is shown in Fig. 3(a). If we choose the following requirement SR $>$ 0.9 as an example, the absolute value of GDD, TOD, and FOD must be less than 163 fs^2, 6700 fs^3, and 90, 200 fs^4, respectively. Figures 3(b) and 3(c) show the pulse contrast when TOD and FOD equal some typical values in order to reveal the relationship between pulse contrast and high-order dispersions. It is demonstrated that pulse contrast of the time point that is several picoseconds ahead of the main pulse is influenced by high-order dispersions, while pulse contrast of the time point that is tens of picoseconds and even several nanoseconds ahead of the main pulse is independent on high-order dispersion for a pulse duration of 30 fs. In laser-plasma interaction experiments such as plasma acceleration of particles, pulse contrast is a crucial parameter. Extremely high contrast of $\sim 10^{-10}$ is required for ultrashort laser with peak power of hundreds of terawatts to petawatts [23]. The typical pulse contrast value of the combined beam could be acquired at 3 ps ahead of the main pulse customarily because all pre-pulse plasma effects start with at least 1–2 ps delay in practical experiments. When TOD and FOD satisfy SR $>$ 0.9, the pulse contrast of the combined beam is better than 10^{-31}, which is a theoretical limit on pulse contrast obtained when one takes into account only the imperfect compression. In real experiment there will be a lot of different effects like amplified spontaneous emission (ASE), parametric fluorescence, stray light from gratings, spectral clipping and so on which will cause this parameter to be much worse.

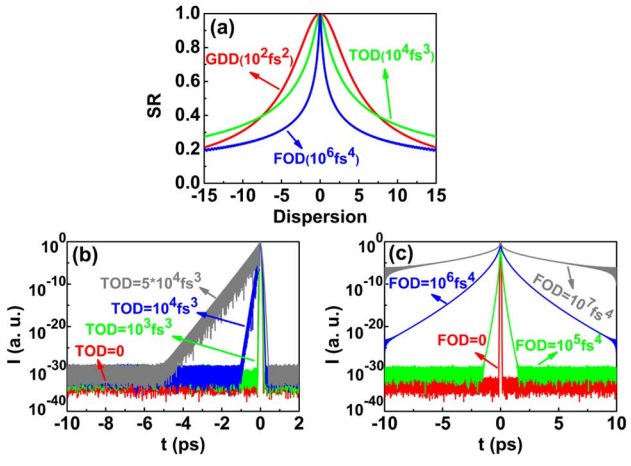

Fig. 3. SR of the combined beam as a function of the individual beam's own GDD, TOD, and FOD (a), temporal intensity of the combined beam on a logarithmic scale for different TOD (b) and FOD (c). The contents in brackets of figure (a) indicate different units for dispersion of different orders.

From the above discussion we can find that the temporal SR degenerates significantly when each beam's own dispersions except GD become greater. And pulse contrast of the combined beam also degenerates considerably when TOD and FOD of each beam turn greater.

B. Control Requirement for the Dispersion Difference

It is clear that residual dispersion makes arriving time or shape of pulse changed. So to some extent the dispersion difference among pulses will inevitably decrease the temporal SR of the combined pulse. First, we discuss a set of typical examples for CBC of two pulses. Here, we let the pulse in Channel 1 has some residual dispersion, while the pulse in Channel 2 has the same or different sign dispersion of pulse 1. The individual intensities for pulses in Channel 1 and 2 and the combined intensity with the same dispersion sign are given in Figs. 4(a)–4(d), while with the same dispersion value but different dispersion sign are represented in Figs. 4(e)–4(h). Taking GDD for example, when the GDD values of the two pulses are opposite in sign, although the intensity shapes of each beam are the same, the temporal intensity of the combined beam reveals beating, which apparently is not expected in CBC for ultrashort pulses. Similar consequences could be found for FOD with opposite sign, as is shown in Fig. 4(h). Figure 4(g) reveals that TOD with different signs brings about oscillations in the combined pulse on its both edges. All of the results in Fig. 4 demonstrate that the peak intensity and pulse shape of the combined beam for dispersion of the same sign are better than that of different dispersion sign even if in the case that the SR of pulse 2 is less. In other words, to realize efficient CBC of two pulses, keeping dispersion values of individual beams with the same sign after dispersion control is a better choice than opposite signs.

It is difficult to generate a pulse without any residual dispersion in real experiments. Now, we assume that the residual dispersion present in Channel 1 make the SR of pulse 1 be 1.0, 0.9, 0.8, 0.7, and 0.6, respectively, the extent to which the pulse in Channel 2 with different dispersions can make the SR of the combined beam be better than 0.9 is considered. As is shown in Fig. 5(a), when group delay is considered, the SR of the combined beam is only related to the difference of GD between the two pulses. From Fig. 5(b), if the SR of pulse 1

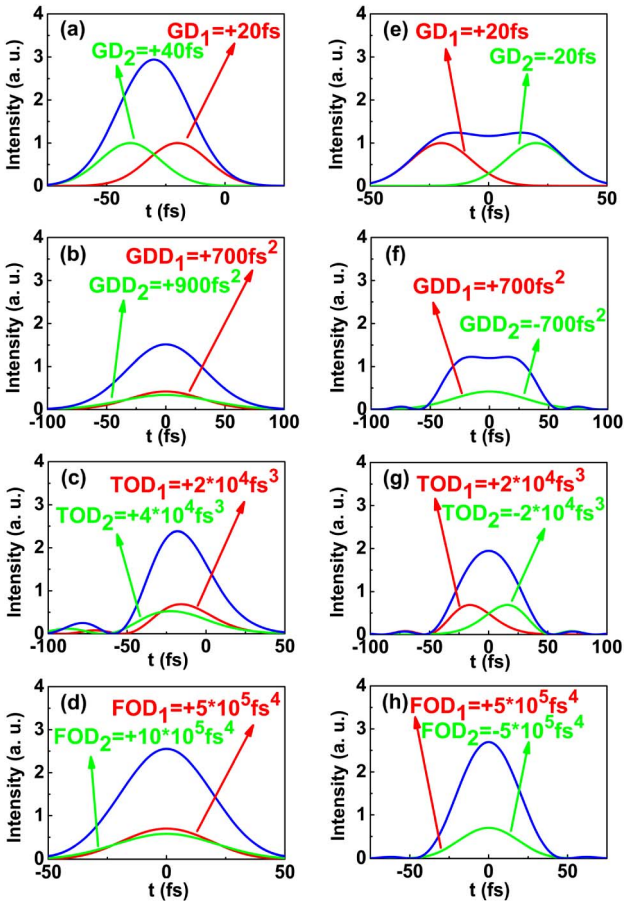

Fig. 4. Intensity profiles for the beams in Channels 1 and 2, and the combined beam with different dispersions with the same sign (a)–(d) and with opposite signs (e)–(h). The red, green, and blue lines denote temporal intensity of the first, second, and combined pulse, respectively.

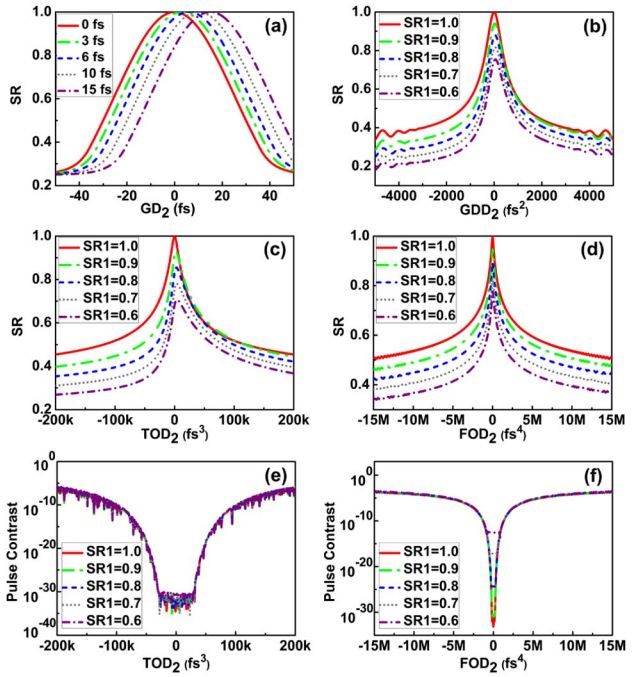

Fig. 5. SR of the combined beam as a function of dispersion in Channel 2 with fixed dispersion of Channel 1, (a) GD_2, (b) GDD_2, (c) TOD_2, and (d) FOD_2. Pulse contrast at 3 ps ahead of the main pulse of the combined beam on a logarithmic scale as a function of (e) TOD_2 and (f) FOD_2.

equals 1, the SR of the combined beam will be the maximum when the dispersions of pulse 2 are zero, which is easily understood. However, if pulse 1 has residual GDD, the SR of the combined beam will decrease as the SR of pulse 1 decreases when pulse 2 has the same GDD. Similar results could be found for TOD and FOD, as is shown in Figs. 5(c) and 5(d). In Figs. 5(e) and 5(f), it is clear that when TOD and FOD of individual pulses are controlled effectively to acquire adequate pulse contrast, pulse contrast of the combined pulse will be adequate naturally; namely, CBC does not influence or even degrade the pulse contrast of the combined beam.

From Fig. 5, we can conclude that the less the SR of pulse 1 is, the more stringent the control requirement for dispersion in pulse 2 can be to get the SR of the combined beam to be larger than 0.9. Unfortunately, if the SR of pulse 1 with residual dispersion is less than 0.8, it is impossible to make SR of the combined beam be larger than 0.9, even when pulse 2 is ideal. So, to realize efficient CBC, the dispersion of each beam should be controlled simultaneously.

C. Multiple Channel Combination

Here, the influence of standard normal random distributions of dispersion and the number of channels to be combined on the SR and pulse contrast of the combined beam are analyzed with Monte Carlo simulations. Assuming dispersion of individual beams to be independent standard normal random variables with mean 0, σ_{GD}, σ_{GDD}, σ_{TOD}, and σ_{FOD} are the root mean squared (rms) instability of parameters GD, GDD, TOD, and FOD, respectively. For every sampling point, we choose 100 values randomly. The SR of the combined beam averaged on random dispersions is performed with numerical simulation. Results of the first-, second-, third-, and fourth-order dispersion coefficient influence on the SR of the combined beam are presented in Figs. 6(a)–6(d), and the effects of the third- and fourth-order dispersion on pulse contrast of the combined beam located at 3 ps ahead of the main pulse are shown in Figs. 6(e)–6(f). The lines of different colors in Fig. 6 correspond to different numbers of channels. For $\tau = 30$ fs, to acquire SR > 0.9 of the combined beam, σ_{GD} must be less than 6.0 fs corresponding to the number of channels $N = 64$, and the σ_{GDD}, σ_{TOD}, and σ_{FOD} must be less than 138 fs^2, 4191 fs^3, and 160, 634 fs^4, respectively. The high-order dispersion control requirements do not vary significantly with the number of the channels to be combined. It is also found that pulse contrast of the combined beam degrades rapidly as σ_{TOD} and σ_{FOD} increase. The reason is that TOD and FOD have a large effect on beam shape, and it should be minimized to limit the intensity oscillations. The process of CBC will not degrade the temporal contrast of the combined beam. When the temporal contrast of individual beams is controlled effectively, pulse contrast of the combined pulse needs no additional control at all, and this is an exciting result for CBC in ultrashort ultrahigh intensity laser systems.

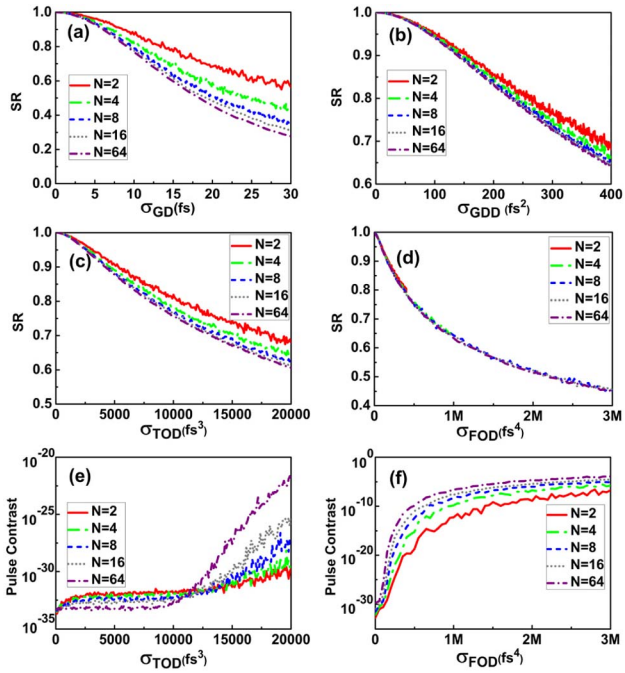

Fig. 6. Dependence of the SR of the combined beam on σ_{GD} (a), σ_{GDD} (b), σ_{TOD} (c), and σ_{FOD} (d), and pulse contrast at 3 ps ahead of the main pulse of the combined beam on a logarithmic scale on σ_{TOD} (e) and σ_{FOD} (f) for different numbers of channels.

The above discussions are limited in a pulse duration of 30 fs. Here we extend the specific system to general ones. The dispersion control requirements of pulses to be combined with different pulse durations have similar results according to numerical simulations, namely SR of the combined pulse as functions of σ_{GD}/τ, σ_{GDD}/τ^2, σ_{TOD}/τ^3, and σ_{FOD}/τ^4 are the same, respectively. The shorter the pulse duration, the more rigid the requirement for dispersion control has to be. For the combined number of 64, σ_{GD}/τ, σ_{GDD}/τ^2, σ_{TOD}/τ^3, and σ_{FOD}/τ^4 of individual pulses should be preserved less than 0.200, 0.153, 0.155, and 0.198, respectively, to realize temporal SR of the combined beam larger than 0.9.

Efficient CBC of ultrashort ultrahigh intensity laser systems requires that residual dispersions of pulses should be compensated effectively. The methods include classical grating double, prism double, acousto-optic programmable dispersive filter, and so on. In view of the current state-of-the-art situation, the core and difficulty of the control requirement in real systems is the group delay, which is influenced by many environmental factors, while GDD, TOD, and FOD could be compensated and controlled statically.

4. SPACE–TIME EFFECTS

In the above discussion we have neglected spatial aspects, which are of great importance to design an efficient ultrashort ultrahigh intensity beam-combining system. In a large aperture ultrashort ultrahigh intensity laser system with pulse duration of 100 fs or larger based on techniques of CPA or OPCPA, lenses are generally important optical elements. For instance, high-energy Petawatt projects (Omega-EP, PETAL) use spatial filters, which are formed with a pair of lenses in their amplifier section to image relay and clear the beam of detrimental spatial frequency modulations. Owing to the inevitable material dispersion introduced by the lens, an ultrashort pulse with large spectral bandwidth has multiple focuses, corresponding to different wavelengths. This is well known as longitudinal chromatism, which induces temporal delay and thus distorts the ultrashort pulse spatially and temporally after focusing.

The theory model of the space–time coupling is as follows. The chromatism could be regarded as the time delay between the rays propagating through, respectively, the edges and the center of the lens in the time domain. The pulse time delay (PTD) of a singlet lens is [24,25]

$$T_{\mathrm{PTD}} = \frac{-\lambda_0}{2cf_0(n_0-1)}\left.\frac{dn}{d\lambda}\right|_{\lambda_0} r_{\max}^2, \tag{10}$$

where n_0, $\left.\frac{dn}{d\lambda}\right|_{\lambda_0}$ are the refractive index and dispersion of the lens material at the central wavelengths λ_0. $r_{\max}$, f_0, and c are the beam size, focal length of the lens, and the optical speed in vacuum, respectively. Equation (10) considers only the first-order derivative of the refractive index, and it is effective in the case of a pulse that is not much shorter than 100 fs, where the PTD is the dominant effect for the coupling between temporal, spectral, and spatial properties of pulses. For pulses with a duration shorter than 100 fs, the group-velocity dispersion (GVD) in the lens material should be considered.

Longitudinal chromatism is another important factor for CBC in large-aperture ultrashort ultrahigh intensity laser systems. However, it has not been discussed systematically in previous works. To reveal the influence process and acquire the PTD control requirement for realizing efficient CBC, the impact of the PTD on the pulse temporal characteristics and spatial distribution at the focus are analyzed based on Fourier optics. In light of actual large-aperture ultrashort ultrahigh intensity laser systems, the parameters of the numerical simulation model are set as follows: the ultrashort pulses centered at 800 nm are Gaussian-shaped in the time domain, and the pulse duration is 300 fs. The aperture of each beam is Φ150 mm, and the spatial distribution of each beam is flat hat top. The focal length of lens is 6.5 m. For simplification, we first consider the combination of two beams.

A. Effect of Pulse Time Delay in Each Pulse on the Combined Beam

First we assume two pulses with the same PTD to be combined. The intensity distribution of the combined beam at the focal plane varies with a different PTD, as is shown in Fig. 7. The intensity $I(r, t)$ at the focal plane is depicted versus r and t, where r is the spatial coordinate and t is the temporal coordinate. It is clear that in the nondispersive case the pulse duration of the combined beam in the vicinity of the focus remains nearly unchanged compared to that of the input individual pulses. With an increasing PTD, the temporal broadening of the combined pulse in the vicinity of the optical axis increases rapidly. Additionally, the spatial distribution changes with time, indicating the coupling of the temporal and spatial properties of the combined pulse. The temporal stretching is a result of the delay between partial pulses that pass through different parts of the lens aperture.

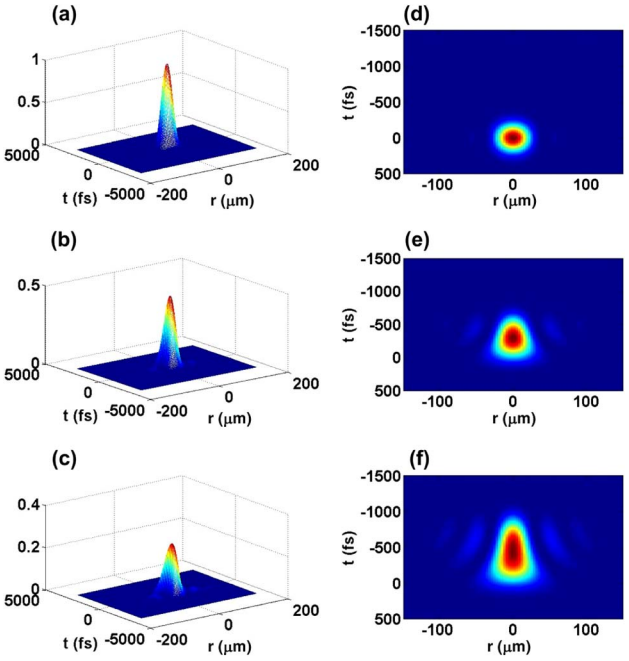

Fig. 7. 3D intensity distribution $I(r, t)$ of the combined beam at the focal plane for various ratios PTD/τ_0 (a) 0, (b) 2, and (c) 3. The pictures (d)–(f) are 2D intensity of (a)–(c), respectively. τ_0 is the ideal pulse duration.

The time-dependent intensity $I(t)$ of the combined beam, derived from spatially integrated $I(r, t)$, is depicted in Fig. 8(a) for various ratios of PTD/τ_0. It is evident that the chromatic aberration of a lens leads to a drastic broadening of the combined pulse form, especially in its front. The pulse width increases and the temporal SR of the combined beam decreases as the ratio PTD/τ_0 increases. The energy density of the combined pulse at the focal plane is shown in Fig. 8(b). Apparently, there is only a small spatial broadening in the focal plane, but the spatial SR decreases significantly as the ratio PTD/τ_0 increases. Moreover, an increasing part of the combined pulse is contained in the wings of the distribution as the ratio PTD/τ_0 increases. The pulse stretching in the time domain and the energy density decreasing in the space domain reduce the peak intensity of the combined beam at focus significantly. To control both the temporal and the spatial SR > 0.8 for CBC of two beams, the PTD of each beam should be no more than τ_0.

B. Pulse Time Delay Difference between Pulses

Now, we assume that the PTD of pulse in Channel 1 is fixed to 0, 0.5, 1, 2, and 3 times the pulse duration, respectively, and consider the extent to which the pulse in Channel 2 with a different PTD can make both the temporal and spatial SR of the combined beam be larger than 0.9. As is shown in Fig. 9, when the PTD of pulse 1 is 0, namely, pulse 1 is ideal, the temporal and spatial SR of the combined pulse will decrease as the PTD of pulse 2 increases. When pulse 1 has a residual PTD, the temporal and spatial SR of the combined pulse will increase up to a maximum at first and decrease afterward as the PTD of pulse 2 increases. The reason may lie in that a small PTD of pulse 2 makes the two pulses overlap both in time domain and spatial domain better than the case of $PTD_2 = 0$. However, after reaching the maximum, the SR will decrease significantly with PTD_2 increasing due to the temporal and spatial distortion of pulse 2, and thus the greater PTD difference between the two pulses.

Clearly, the larger the PTD of pulse 1 is, the more rigid the control requirement can be for the PTD in pulse 2 to get the SR of the combined beam >0.9. If the PTD of pulse 1 equals pulse duration, it is impossible to make the SR of the combined beam larger than 0.9, even if pulse 2 is ideal. So, to realize efficient beam combining of two pulses, the PTD of each beam should be effectively controlled to be less than 1 time pulse duration simultaneously.

C. Multiple Channel Combination

Similarly, we analyze the influence of standard normal random distributions of the PTD, and the number of the channels to be combined on the temporal and spatial SR of the combined beam with Monte Carlo simulations. Assuming a PTD of individual beams to be independent standard normal random variables and the mean value to be 0, the temporal and spatial SR of the combined beam averaged on a random PTD with 100 values is performed by numerical simulation. σ_{PTD} is the rms instability of parameter PTD.

Results of the PTD influence on temporal and spatial SR of the combined beam are shown in Fig. 10. For CBC of two pulses, to acquire temporal and spatial SR > 0.9 of the combined beam, σ_{PTD} must be less than 0.7 times the pulse duration. When the number of channel increases to 4, σ_{PTD} must be less than 0.4 times of the pulse duration. Fortunately, the channel number's further increasing does not raise the control requirement of the PTD.

Now the influence of GVD on the temporal and spatial characteristics of pulses in the focal plane with duration shorter than 100 fs is added. The pulse width is assumed to be 30 fs for numerical simulation. The results are shown in Fig. 11. To make temporal and spatial SR be larger than 0.9 of the

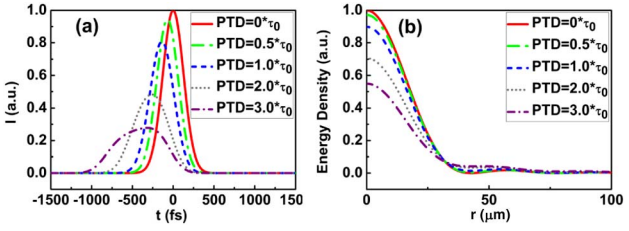

Fig. 8. (a) $I(t)$ and (b) energy density of the combined beam with different PTD/τ_0.

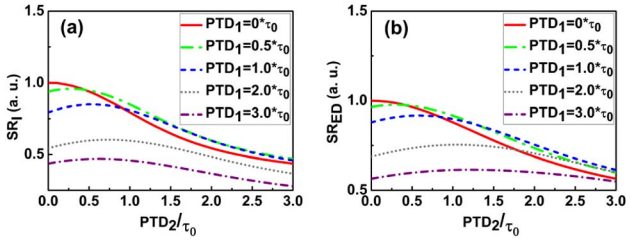

Fig. 9. Temporal SR of the combined beam (a) and a spatial SR (b) as a function of PTD_2/τ_0. ED denotes energy density.

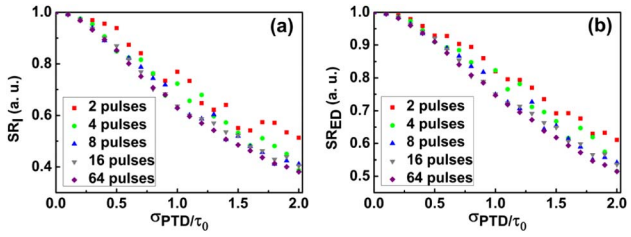

Fig. 10. Dependence of the temporal SR (a) and spatial SR (b) of the combined beam on σ_{PTD}. Different symbols of different colors correspond to different numbers of channels to be combined.

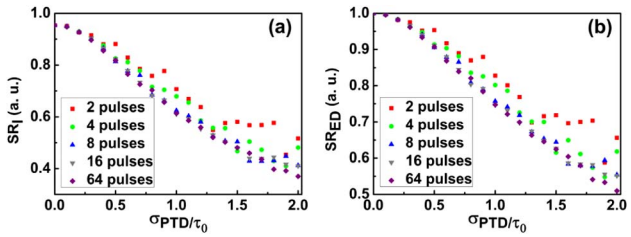

Fig. 11. Dependence of the temporal SR (a) and spatial SR (b) of the combined beam on σ_{PTD} considering GVD. Different symbols of different colors correspond to different numbers of channels to be combined.

combined beam, σ_{PTD} must be less than 0.3 times the pulse duration. Evidently, the control requirement is more stringent than the case that GVD is neglected. The reason lies in that once GVD plays a part, the pulses become broadened further and experience a larger reduction in temporal SR of the combined beam owing to a superposition of partial pulses with different durations and peak intensities in the focal plane. However, GVD has little influence on the energy density distribution of a pulse in the focal plane. Higher-order dispersions of a lens play a relatively minor role, and they are neglected.

To realize efficient CBC of ultrashort ultrahigh intensity laser systems, longitudinal chromatism should be compensated or avoided effectively for different pulse durations. The solutions include classical achromats, diffractive optics, reflective optical elements, and so on. It should be pointed out that for laser systems with a pulse duration of less than 10 fs, only reflective telescopes for the signal beam are used due not only to chromatic aberrations but also to nonlinear phase distortions in the lens. The nonlinear phase distortion is not considered here.

5. CONCLUSIONS

To get the general spectral control requirements of CBC for ultrashort ultrahigh intensity laser systems, factors such as spectral dispersions and longitudinal chromatism are analyzed. Different orders of dispersion will influence the intensity shape of the combined beam, and high-order dispersions will affect pulse contrast of the combined beam, an important parameter for high-energy physics experiments. For the combined number of 64, σ_{GD}/τ, σ_{GDD}/τ^2, σ_{TOD}/τ^3, and σ_{FOD}/τ^4 of individual pulses should be preserved at less than 0.200, 0.153, 0.155, and 0.198, respectively, to realize a temporal SR of the combined beam larger than 0.9. The number of the channels to be combined has little impact on the SR of the combined beam. Once high-order dispersions of individual pulses are controlled effectively, pulse contrast of the combined beam does not need extra control. Longitudinal chromatism has a detrimental effect on the combined beam in the focal plane, both temporally and spatially, and should be controlled effectively. For CBC of two beams longer than 100 fs, the PTD should be less than 0.7 times the pulse duration to realize efficient beam combining while the PTD must be less than 0.4 times the pulse duration for more channels combining. When GVD is not neglected for a pulse duration shorter than 100 fs, the PTD should be less than 0.3 times the pulse duration for efficient CBC. This paper will provide a reference for designing ultrashort ultrahigh intensity laser systems based on CBC.

Funding. National Natural Science Foundation of China (NSFC) (11604317, 61205137, 11204331, 61308021, 61605190, 11604318, U1330129).

REFERENCES

1. Y. X. Chu, Z. B. Gan, X. Y. Liang, L. H. Yu, X. M. Lu, C. Wang, X. L. Wang, L. Xu, H. H. Lu, D. J. Yin, Y. X. Leng, R. X. Li, and Z. Z. Xu, "High-energy large-aperture Ti:sapphire amplifier for 5 PW laser pulses," Opt. Lett. **40**, 5011–5014 (2015).
2. F. Giambruno, C. Radier, G. Rey, and G. Cheriaux, "Design of a 10 PW (150 J/15 fs) peak power laser system with Ti:sapphire medium through spectral control," Appl. Opt. **50**, 2617–2621 (2011).
3. G. A. Mourou, T. Tajima, and S. V. Bulanov, "Optics in the relativistic regime," Rev. Mod. Phys. **78**, 309–371 (2006).
4. S. V. Bulanov, T. Z. Esirkepov, M. Kando, J. Koga, K. Kondo, and G. Korn, "On the problems of relativistic laboratory astrophysics and fundamental physics with super powerful lasers," Plasma Phys. Rep. **41**, 1–51 (2015).
5. A. Lyachev, O. Chekhlov, J. Collier, R. J. Clarke, M. Galimberti, C. Hernandez-Gomez, P. Matousek, I. O. Musgrave, D. Neely, P. A. Norreys, I. Ross, Y. Tang, T. B. Winstone, and B. E. Wyborn, "The 10 PW OPCPA Vulcan laser upgrade," in *High Intensity Lasers and High Field Phenomena (HILAS)*, Istanbul, 2011, paper HThE2.
6. S. N. Bagayev, V. E. Leshchenko, V. I. Trunov, E. V. Pestryakov, and S. A. Frolov, "Coherent combining of femtosecond pulses parametrically amplified in BBO crystals," Opt. Lett. **39**, 1517–1520 (2014).
7. P. F. Ma, R. M. Tao, X. L. Wang, Y. X. Ma, R. T. Su, and P. Zhou, "Coherent polarization beam combination of four mode-locked fiber MOPAs in picosecond regime," Opt. Express **22**, 4123–4130 (2014).
8. L. Lombard, A. Azarian, K. Cadoret, P. Bourdon, D. Goular, G. Canat, V. Jolivet, Y. Jaouën, and O. Vasseur, "Coherent beam combination of narrow-linewidth 1.5 μm fiber amplifiers in a long-pulse regime," Opt. Lett. **36**, 523–525 (2011).
9. E. Seise, A. Klenke, S. Breitkopf, M. Plötner, J. Limpert, and A. Tünnermann, "Coherently combined fiber laser system delivering 120 μJ femtosecond pulses," Opt. Lett. **36**, 439–441 (2011).
10. B. Rus, P. Bakule, D. Kramer, G. Korn, J. T. Green, J. Nóvak, M. Fibrich, F. Batysta, J. Thoma, and J. Naylon, "ELI-beamlines laser systems: status and design options," Proc. SPIE **8780**, 87801T (2013).
11. "Exawatt center for extreme light studies (XCELS), project summary," http://www.xcels.iapras.ru/img/site-XCELS.pdf.
12. G. D. Goodno, C. C. Shih, and J. E. Rothenberg, "Perturbative analysis of coherent combining efficiency with mismatched lasers," Opt. Express **18**, 25403–25414 (2010).
13. V. E. Leshchenko, "Coherent combining efficiency in tiled and filled aperture approaches," Opt. Express **23**, 15944–15970 (2015).
14. Y. Q. Gao, W. X. Ma, B. Q. Zhu, D. Z. Liu, Z. D. Cao, J. Zhu, and Y. P. Dai, "Phase control requirement of high intensity laser beam combining," Appl. Opt. **51**, 2941–2950 (2012).

15. Z. X. Zhao, Y. Q. Gao, Y. Cui, Z. Y. Xu, N. An, D. Liu, T. Wang, D. X. Rao, M. Chen, W. Feng, L. L. Ji, Z. D. Cao, X. D. Yang, and W. X. Ma, "Investigation of phase effects of coherent beam combining for large-aperture ultrashort ultrahigh intensity laser systems," Appl. Opt. **54**, 9939–9948 (2015).
16. A. Klenke, E. Seise, J. Limpert, and A. Tünnermann, "Basic considerations on coherent combining of ultrashort laser pulses," Opt. Express **19**, 25379–25387 (2011).
17. D. Homoelle, J. K. Crane, M. Shverdin, C. L. Haefner, and C. W. Siders, "Phasing beams with different dispersions and application to the petawatt-class beamline at the national ignition facility," Appl. Opt. **50**, 554–561 (2011).
18. L. Daniault, M. Hanna, L. Lombard, Y. Zaouter, E. Mottay, D. Goular, P. Bourdon, F. Druon, and P. Georges, "Impact of spectral phase mismatch on femtosecond coherent beam combining systems," Opt. Lett. **37**, 650–652 (2012).
19. S. F. Jiang, M. Hanna, F. Druon, and P. Georges, "Impact of self-phase modulation on coherently combined fiber chirped-pulse amplifiers," Opt. Lett. **35**, 1293–1295 (2010).
20. R. T. Su, P. Zhou, X. L. Wang, H. W. Zhang, and X. J. Xu, "Impact of temporal and spectral aberrations on coherent beam combination of nanosecond fiber lasers," Appl. Opt. **52**, 2187–2193 (2013).
21. S. Backus, C. G. Durfee, M. M. Murnane, and H. C. Kapteyn, "High power ultrafast lasers," Rev. Sci. Instrum. **69**, 1207–1223 (1998).
22. M. Miyagi and S. Nishida, "Pulse spreading in a single-mode fiber due to third-order dispersion," Appl. Opt. **18**, 678–682 (1979).
23. T. J. Yu, S. K. Lee, J. H. Sung, J. W. Yoon, T. M. Jeong, and J. Lee, "Generation of high-contrast, 30 fs, 1.5 PW laser pulses from chirped pulse amplification Ti:sapphire laser," Opt. Express **20**, 10807–10815 (2012).
24. H. M. Heuck, P. Neumayer, T. Kuhl, and U. Wittrock, "Chromatic aberration in petawatt-class lasers," Appl. Phys. B **84**, 421–428 (2006).
25. M. Kempe, U. Stamm, B. Wilhelmi, and W. Rudolph, "Spatial and temporal transformation of femtosecond laser pulses by lenses and lens system," J. Opt. Soc. Am. B **9**, 1158–1165 (1992).